NDT&E International 64 (2014) 1–6

Contents lists available at ScienceDirect

NDT&E International

journal homepage: www.elsevier.com/locate/ndteint

# Impedance of a curved circular spiral coil around a conductive cylinder

S.K. Burke [a], R.J. Ditchburn [a,*], T.P. Theodoulidis [b]

[a] Defence Science and Technology Organisation, Fishermans Bend, VIC 3207, Australia
[b] Department of Mechanical Engineering, University of Western Macedonia, Kozani 50100, Greece

ARTICLE INFO

*Article history:*
Received 15 October 2013
Received in revised form
29 January 2014
Accepted 13 February 2014
Available online 20 February 2014

*Keywords:*
Coils
Eddy currents
Impedance
Inductance
Theoretical modeling

ABSTRACT

Expressions are presented for the inductance of a curved circular spiral coil in free space and the change in impedance when the coil is wrapped around the surface of a magnetic, conductive cylinder. Inductance and impedance measurements of a thin conformable coil on a cylindrical Al-alloy rod were used to test the validity of these expressions. The theoretical predictions are in very good agreement with the experimental measurements over the frequency range 1 kHz–10 MHz. The findings are compared with previous work using rectangular spiral coils and it was found that the change in normalized impedance at high frequencies for a circular coil was almost identical to that obtained for a similarly-sized square coil. The implications for use in eddy-current nondestructive testing are discussed.


## 1. Introduction

A range of thin, conformable eddy-current sensors has been developed for crack detection and materials characterization applications over the past 20 years [1–6]. The principal advantage of such sensor coils is that higher inductive coupling can be achieved through the combination of smaller coil liftoff and better conformation to a highly curved surface than can be achieved with conventional rigid wire-wound coils. Another advantage is that multi-coil arrays of such thin sensor coils can be readily fabricated using flexible printed-circuit board technology to allow increased inspection coverage and options for in-situ monitoring [7–12].

An inherent drawback of thin coils is their low inductance which means that the coils often need many windings resulting in a larger footprint and decreased position resolution for defect detection than conventional coils. The lower inductance also limits the lower frequency application of such sensors for the detection of buried defects. However, for many applications this is not important.

In a previous paper [13], the impedance of a curved rectangular coil around a conductive cylinder was studied experimentally and theoretically using a second-order vector potential (SOVP) formalism. Here the same approach is adopted to investigate a curved circular coil around a conductive cylinder. The motivation for the present work was to investigate the potential role of the curved spiral coil geometry on eddy-current response. The theoretical and experimental results for the curved circular coil are compared to those for a similarly-sized curved square coil and the implications for use in eddy-current nondestructive testing are discussed.

## 2. Theory

### 2.1. Configuration

The configuration is shown in Fig. 1, where a thin planar spiral coil with $N$ equally spaced circular turns is wrapped around a conductive cylinder with radius $b$. The coil has an inner radius $r_1$, outer radius $r_2$ and is separated from the surface of the cylinder by a constant lift-off $h$ to give a radius of curvature of $a=b+h$ for the coil. The cylinder has an electrical conductivity $\sigma$, relative magnetic permeability $\mu_r$ and is assumed to have infinite length. The coil is excited by an alternating current $I\exp(j\omega t)$ where $\omega=2\pi f$ and $f$ is the excitation frequency.

In the following, a cylindrical polar coordinate system $(\rho,\varphi,z)$ will be used with the $z$ axis along the cylinder axis. With this coordinate system, the coil center lies at a position $(a,0,0)$ and the curved surface of the coil is located on the cylindrical surface $\rho=a$.

### 2.2. Impedance change for a curved circular spiral coil around a conductive cylinder

The general expression for the impedance change $\Delta Z$ for an arbitrary air-cored coil due to eddy-current induction in an infinitely long cylinder has been given previously [13,14],

$$\Delta Z=\frac{4\pi^2 j\omega}{\mu_0 I^2}\int_{-\infty}^{\infty}\alpha^2\sum_{m=-\infty}^{\infty}C_s(-\alpha,-m)C_s(\alpha,m)R(\alpha,m)d\alpha. \tag{1}$$

* Corresponding author. Tel.: +61 3 9626 7518.
*E-mail address:* rob.ditchburn@dsto.defence.gov.au (R.J. Ditchburn).

http://dx.doi.org/10.1016/j.ndteint.2014.02.002

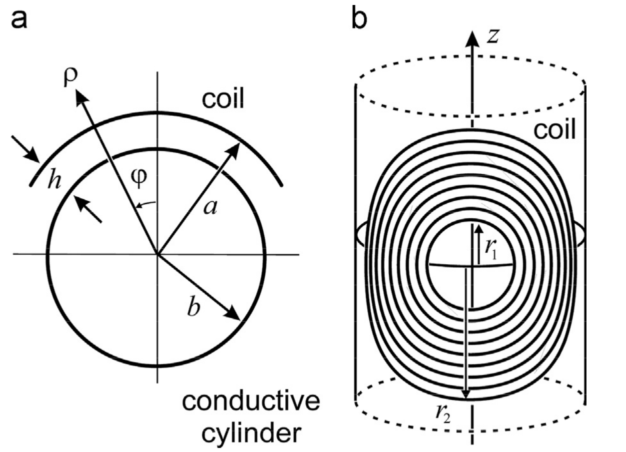


**Fig. 1.** Curved circular spiral coil wrapped around an infinitely long conductive cylinder (schematic). (a) End view and (b) side view.

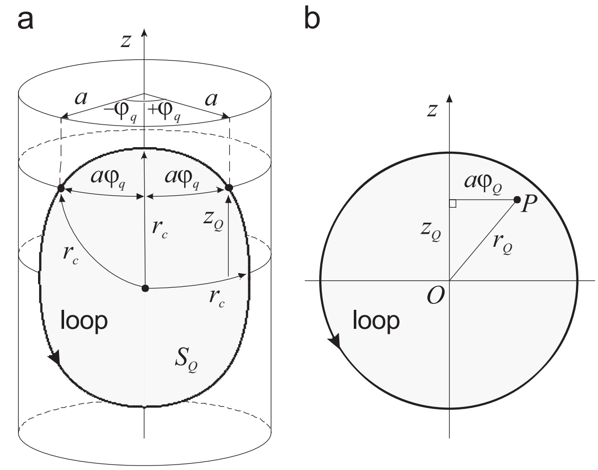


**Fig. 2.** Curved circular loop with cylindrical curvature. (a) Geometry used for the calculation of the source coefficient for a single curved loop. (b) Loop unwrapped from the cylinder showing an arbitrary point $P$ on the loop surface and the construction leading to Eq. (7).

The coil geometry appears through the source coefficient $C_s$ and the electromagnetic properties of the conductive cylinder enter through the reflection coefficient

$$R(\alpha,m)=\frac{I_m(|\alpha|b)}{K_m(|\alpha|b)}\times\frac{k^2m^2\mu_r+\alpha_1^2b^2\Lambda(\alpha_1 b)[\alpha^2\mu_r\Lambda(\alpha_1 b)-|\alpha|\alpha_1\Lambda(|\alpha|b)]}{k^2m^2\mu_r+\alpha_1^2b^2\Lambda(\alpha_1 b)[\alpha^2\mu_r\Lambda(\alpha_1 b)-|\alpha|\alpha_1 M(|\alpha|b)]}, \quad (2)$$

where $k^2=j\omega\mu_0\mu_r\sigma$, $\alpha_1^2=\alpha^2+k^2$, $\mu_0$ is the permeability of free-space and

$$\Lambda(x)=\frac{I'_m(x)}{I_m(x)}=\frac{m}{x}+\frac{I_{m+1}(x)}{I_m(x)}, \quad (3)$$

$$M(x)=\frac{K'_m(x)}{K_m(x)}=\frac{m}{x}-\frac{K_{m+1}(x)}{K_m(x)}. \quad (4)$$

Here $I_m$ and $K_m$ denote modified Bessel function of the first and second kind respectively, with derivatives $I'_m$ and $K'_m$.

To derive an explicit formula for $\Delta Z$ in the specific case of a curved circular spiral coil, the correct expression for the source coefficient $C_s$ must first be obtained. The required closed-form expression for $C_s$ can be constructed by first considering the source coefficient for a single curved current loop and then superposing the results to construct $C_s$ for the complete coil.

### 2.2.1. *Source coefficient for a single curved loop*

Adapting the results of [13,15,16], the source coefficient due to an arbitrary current loop in free space can be expressed in terms of a surface integral over an arbitrary surface $S_Q$ bounded by the loop,

$$C_s^{loop}=\frac{\mu_0 I}{(2\pi)^2}\frac{j}{\alpha}\iint_{S_Q}\hat{\mathbf{n}}\cdot\nabla_Q[K_m(|\alpha|\rho_Q)e^{-jm\varphi_Q}e^{-j\alpha z_Q}]\,dS, \quad (5)$$

where the coordinates $(\rho_Q, \varphi_Q, z_Q)$ denote a point lying on $S_Q$, the gradient operator applies to these surface coordinates and $\hat{\mathbf{n}}$ is the unit outward vector normal to $S_Q$.

The curved circular spiral coil is assumed to be made up by a series of individual curved loops shown in Fig. 2(a). Each loop takes the form of a circle of radius $r_c$ which is wrapped over the cylinder. To compute $C_s^{loop}$ using the general expression Eq. (5), $S_Q$ is chosen to be the curved surface of the loop ($\rho_Q=a$, $|z_Q|\le r_c$, $|\varphi_Q|\le+\varphi_q$) and $\hat{\mathbf{n}}=\hat{\rho}$. With this choice, only the $\rho$ component of the gradient operator remains and Eq. (5) reduces to the integral

$$C_s^{loop}=\frac{j\mu_0 I a}{(2\pi)^2}\mathrm{sgn}(\alpha)K'_m(|\alpha|a)\int_{-r_c}^{+r_c}\int_{-\varphi_q}^{+\varphi_q}e^{-jm\varphi_Q}e^{-j\alpha z_Q}\,d\varphi_Q\,dz_Q. \quad (6)$$

The limits of integration in Eq. (6) can be determined from the geometry by noting that the distance $r_Q$ measured along the curved loop surface from the center of the loop $(a,0,0)$ to an arbitrary point $P$ $(a, \varphi_Q, z_Q)$ on the curved loop surface is given by

$${z_Q}^2+(a\varphi_Q)^2=r_Q^2. \quad (7)$$

Eq. (7) follows from the application of Pythogoras' theorem after unwrapping the curved surface of the loop as shown in Fig. 2 (b). Hence, on the boundary of the loop, $r_Q=r_c$, and $\varphi_q$ which appears in the integration limits for Eq. (6) is

$$\varphi_q(z_Q)=\frac{1}{a}\sqrt{r_c^2-{z_Q}^2}, \quad (8)$$

where the dependence on $z_Q$ is shown explicitly. Performing the double integration, Eq. (6) reduces to the expression

$$C_s^{loop}=\frac{j\mu_0 I}{2\pi}\mathrm{sgn}(\alpha)\frac{r_c J_1(r_c\sqrt{{\nu_m}^2+\alpha^2})}{\sqrt{\nu_m^2+\alpha^2}}K'_m(|\alpha|a), \quad (9)$$

where $\nu_m=m/a$, $J_1$ is a first order Bessel function and §3.711 of Gradshteyn and Ryzhik [17] has been used to evaluate the final integral over $z$.

### 2.2.2. *Source coefficient for a curved circular spiral coil*

The source coefficient $C_s$ for the complete coil can now be constructed by superposition of the source coefficient Eq. (9) for $N$ individual loops. Using a continuum approximation, the sum over the $N$ discrete turns can be replaced by the integral

$$C_s=n_d\int_{r_1}^{r_2}C_s^{loop}dr_c, \quad (10)$$

where $n_d$ is the turn density of the coil $N/(r_2-r_1)$. Substituting Eq. (9) into Eq. (10) and evaluating the integral over $r_c$ gives the final expression

$$C_s(\alpha,m)=j\frac{\mu_0 IN}{2\pi(r_2-r_1)}\frac{\mathrm{sgn}(\alpha)}{(\nu_m^2+\alpha^2)^{3/2}}J(r_1\sqrt{\nu_m^2+\alpha^2},r_2\sqrt{\nu_m^2+\alpha^2})K'_m(|\alpha|a), \quad (11)$$

where

$$J(x_1,x_2)=\int_{x_1}^{x_2}xJ_1(x)dx=\frac{\pi x_2}{2}[J_1(x_2)H_0(x_2)-J_0(x_2)H_1(x_2)]-\frac{\pi x_1}{2}[J_1(x_1)H_0(x_1)-J_0(x_1)H_1(x_1)], \quad (12)$$